Sādhanā Vol. 42, No. 10, October 2017, pp. 1773–1781
DOI 10.1007/s12046-017-0717-6 © Indian Academy of Sciences

Property elucidation of vacuum-evaporated zinc telluride thin film towards optoelectronic devices

J U AHAMED[1,*], N P BEGUM[1] and M N I KHAN[2]

[1]Department of Applied Physics, Electronics and Communication Engineering, University of Chittagong, Chittagong 4331, Bangladesh
[2]Materials Science Division, Atomic Energy Center, Dhaka, Bangladesh
e-mail: ahamed.jamal@cu.ac.bd

MS received 2 August 2016; revised 14 January 2017; accepted 9 March 2017; published online 31 August 2017

Abstract. A thermal vacuum evaporation system has been used to deposit zinc telluride (ZnTe) thin film on glass substrate in order to investigate the structural, morphological, optoelectronic and electrical properties of the deposited film. The deposited film has been characterised by X-ray diffraction (XRD), atomic force microscopy (AFM), and UV-VIS-NIR spectrophotometer. The polycrystalline and cubic structure of the sample has been confirmed by XRD. The order parameter(s), which determines the crystallinity and good environmental stability of the sample, has been obtained for the peak (1 1 1) to peak (2 0 0) and is found to be 0.83. The XRD patterns and Bragg's law have been examined to determine the microstructural parameters (lattice parameter, inter-planar spacing, crystallite size, number of crystallites per unit area, strain, dislocation density) of the investigated film. Optical properties (transmittance, absorbance, refractive index, absorption coefficient, extinction coefficient, optical density) of ZnTe thin film were extensively studied in incident photon energy range of 0.5–3.5 eV, where direct optical transition has been obtained with a band gap of 2.63 eV. The surface morphology of the evaporated ZnTe thin film has been checked by AFM.

Keywords. Order parameter; crystallite size; surface morphology; dislocation density; absorption coefficient; extinction coefficient.

1. Introduction

Polycrystalline, semiconducting, binary metal chalcogenide materials belonging to II–VI groups have emerged a rapidly increasing area of research due to their potential applications in a variety of solid-state devices. Wide-gap II–VI compound semiconductors are particularly efficient electroluminescence materials (ELs) as compared to III–V compounds because of their nature of indirect band gap. On the other hand, all IIb–VIb compounds are direct band-gap materials and they are chemically stable and show high luminescence. Additionally, the high ionicity of these compounds makes them good candidates for high optoelectronics and electro-optical coupling. Zinc telluride (ZnTe) is one of the promising semiconducting materials for solid-state optoelectronics devices (photo-detectors, photovoltaic solar cells, light-emitting diodes, laser diodes, microwave devices, thermoelectric devices, etc.) because of its size-dependent characteristics, large band gap, low resistivity and high transparency in visible spectral domain [1–3]. The optical properties of ZnTe can be tuned by changing their structure or composition. It is an intrinsically p-type semiconductor due to its non-stoichiometric (Zn vacancy) characteristic with an ideal band gap of 2.26 eV [3]. This type of material ensures high transparency in the visible spectral range and is widely used in multi-junction tandem solar cells. The photovoltaic (solar energy to electricity) activity of ZnTe homojunction diodes showed open-circuit voltage of 0.9 V under one-sun intensity [4]. Furthermore, ZnTe is a promising material for the fabrication of purely green light-emitting diode, THz emitters, switching devices and buffer layers for HgCdTe IR detectors [5–7]. A variety of vapor-phase and solution-based techniques are available for the deposition of ZnTe thin films. These include vacuum evaporation, sputtering, electron beam evaporation, chemical bath deposition (CBD), molecular beam epitaxy (MBE), and close space sublimation (CSS) techniques [8–13]. A much smaller band gap of 1.0 eV is reported for the laser-ablated films and much larger values (2.62–3.24 eV) have been observed for vacuum-evaporated films [14, 15].

Here we discuss the importance of vacuum evaporation method for the deposition of ZnTe thin film as compared to other methods. At first, the comparison was made with pulsed laser deposition technique. The pulsed laser deposition technique is a physical vapor deposition (PVD)

*For correspondence

similar to vacuum evaporation, but it is very complex, expensive and requires ultra-high vacuum as compared to the vacuum evaporation technique. Splashing is an intrinsic problem that is difficult to overcome and a major drawback of pulsed laser deposition [16]. Secondly, a comparison was made with the sputtering process. Sputter deposition, for polycrystalline films, produces the film grain structure that has typically many crystallographic orientations without a preferred texture [17]. However, kinetic energy of sputtered atoms in sputter deposition is higher than that of atoms in the evaporative deposition because of the argon gas (Ar) existence in the sputtering system. Therefore, the surface of deposition in sputtering process exhibits more damage and defective nucleation than in thermal evaporation. Based on the advantages and disadvantages of different deposition process, it was found that vacuum evaporation can be used on a large area and the physical properties of the films can easily be controlled by the deposition conditions (e.g. deposition rate, temperature and thickness) [18]. In addition, kinetic energy of the atoms of the material is low in thermal evaporation, and therefore, the deposition surface is protected from defective nucleation and damage. Hence, it can be concluded that even though there are some drawbacks associated with thermal vacuum evaporation, the benefits probably outweighed the disadvantages.

Although there have been a number of investigations on the ZnTe films by many researchers all over the world, in-depth studies on the structural, morphological, optical and electrical properties of ZnTe thin films are scarce. The structural, optical and electrical properties of semiconductor compounds are drastically affected by impurities and native defects. Hence, this study aimed to better understand the growth mechanisms involved in the formation of ZnTe thin films and how a growth parameter such as annealing temperature affects their overall properties. The novelty of the present study is to investigate the structural, morphological, optoelectronic and electrical properties of ZnTe thin film and to comprehend the optical behaviors for its utilisation as optically active material in various optoelectronic devices.

In this study, ZnTe thin film has been deposited onto a cleaned glass substrate by vacuum evaporation and annealed at various temperatures in vacuum for 1 h. The deposited film has been characterised by using X-ray diffraction (XRD), and atomic force microscope (AFM). Structural, morphological, optoelectronic and electrical properties of the deposited ZnTe thin film have been investigated.

2. Experimental details

2.1 *Sample preparation*

Zinc telluride thin film has been deposited on to a well-cleaned glass substrate with the help of a high vacuum coating unit (Edwards, UK, and Model E306A) under vacuum of 10^{-5} Torr, as shown in figure 1. Pure (99.99%) ZnTe was used as the source material. The material was placed into a thin tantalum boat used as a source heater. The boat was heated indirectly by passing current through the electrodes.

The glass slide was cleaned with an ultrasonic cleaner and distilled water. The distance between the source and substrate was maintained at 14.5 cm. The substrate temperature was constant at 373 K. The substrate was heated by a spiral resistance heater and the temperature was measured by a chromel–alumel thermocouple placed in the middle of the substrate. Deposition of the film on the substrate was controlled by using a source shutter. When all the parameters (vacuum, rate of deposition, deposition temperature, etc.) were optimised, the source shutter was displaced and film deposited on the substrate. As the as-deposited samples have a high order of resistivity, it is essential to anneal the sample. The annealing temperature must be maintained higher than the evaporation temperature in order to create homogeneous films. Hence, the sample was annealed in vacuum for 1 h at different temperatures of 423 K, 473 K, 523 K and 573 K. In order to avoid contamination and oxidation, the film was allowed to cool down inside the vacuum chamber at room temperature. The thickness of the deposited thin film was estimated as 400 nm.

2.2 *Structural characterisation*

Several methods are available to characterise the structure of semiconductor thin films. X-ray diffraction (XRD), atomic force microscope (AFM), scanning electron microscope (SEM), transmission electron microscope (TEM) and scanning electron microscope (STM) are some of the

Figure 1. Preparation of ZnTe thin film. Sample using high vacuum coating unit (Edwards, U.K., and Model E306A).

widely used methods for structural characterisation [19–22]. XRD studies confirm the compound formation and unit cell parameters, crystallite site [14] etc.

In this present study, the polycrystalline and cubic structure of the sample has been confirmed by XRD. The effect of annealing temperature on the structure of these films is clearly seen from the XRD data. X-ray diffraction measurements have been taken using Philips Pan Analytic X'Pert Pro X-ray diffractometer having CuKα as a radiation source of wavelength $\lambda = 1.5406$ Å with $2\theta = 20^\circ$–70° at the scan speed 0.5°/min for the determination of the structure of the films. The data has been analysed using Powder X program.

AFM measurements were carried out using a scanning probe microscope (using TT-AFM, AFM Workshop, USA) in contact mode. Rectangular cantilevers of silicon nitride (length 200 mm and width 40 mm) having a force constant of 3 N/m were employed for the measurement. Optical properties of the ZnTe thin films were observed out using a UV-VIS-NIR spectrophotometer (Shimadzu, UV-3100PC, Japan). Electrical properties of the prepared samples were measured using four probe methods. All the characteristics were measured at room temperature.

3. Results and discussion

3.1 *Structural properties*

The present work focuses on the influence of annealing temperature on structural, electrical and optical properties of ZnTe thin films. Figure 2 shows the XRD patterns of vacuum-evaporated ZnTe thin film annealed at (a) 423 K, (b) 473 K, (c) 523 K and (d) 573 K respectively. It was found that the diffraction peaks at 2θ angles of 23.87°, 25.47°, 42.79° and 46.62° correspond to (1 1 1), (2 0 0), (2 2 0) and (3 1 1) planes of the cubic structure of the

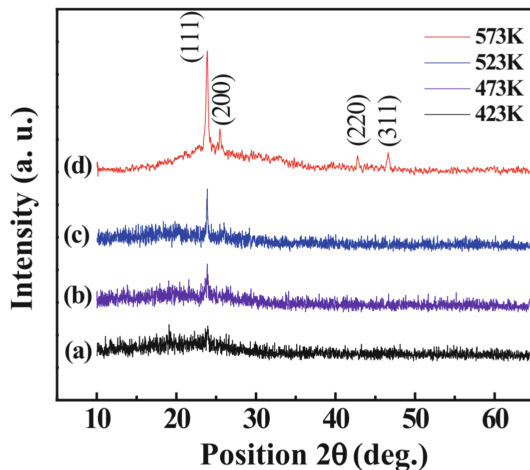

Figure 2. X-ray diffraction patterns for ZnTe thin film annealed at (**a**) 423 K, (**b**) 473 K, (**c**) 523 K, and (**d**) 573 K respectively.

ZnTe. It is evident from figure 2 that the intensity of (1 1 1), (2 0 0), (2 2 0) and (3 1 1) reflection increases with the increase in annealing temperature and becomes sharper on reducing the peak width. It is also observed that the XRD pattern of ZnTe film annealed at 573 K (figure 2d) is polycrystalline in nature, having cubic crystal structure, preferred orientation along (1 1 1) together with other planes (2 0 0), (2 2 0) and (3 1 1). The peak intensity is found to increase with the increase in annealing temperature, which may be due to the enhancement of clusters, rearrangement of atoms and removal of residual stresses/defects formed during the film deposition [23]. Literature report showed that substrate temperature also has an effect on the evaporated thin film; the peak intensity, the number of peaks and the grain size were found to increase with the increase in substrate temperature [24]. Surface morphology of the film is sensitive to annealing temperature; hence, increment of annealing temperature generates microscale surface roughness and the amount of aggregations on the films also increased.

Different diffraction peaks were identified and the corresponding values of inter-planar spacing, d_{hkl} ((hkl) are Millers indices), were calculated from the Bragg equation:

$$n\lambda = 2d_{hkl}\sin\theta. \quad (1)$$

The lattice parameter, 'a' for ZnTe cubic phase structure was determined using the relation:

$$a = d_{hkl} \times \sqrt{h^2 + k^2 + l^2}. \quad (2)$$

The number of crystallites per unit area is determined by using the relation given as follow:

$$N = \frac{t}{D^3}. \quad (3)$$

The crystallite size is determined from XRD data using the Scherrer formula:

$$D = \frac{k\lambda}{\beta\cos\theta} \quad (4)$$

where k is the constant, β is full-width at half-maximum (FWHM) in radians, λ is the wavelength of X-ray used, θ is the Bragg angle. The crystallite size can be increased by increasing the film thickness, so the crystal defects (stacking fault), internal microstrain and dislocation density will be decreased in the lattice [25, 26]. The strain is related to the geometric measure of lattice deformation, which in turn depends on the deposition conditions. Dislocation is an irregularity in a crystal structure associated with the lattice, which in turn depends on the growth mechanisms. The microstrain (ε) and the dislocation density (ρ) of the film were estimated using Eqs. 5 and 6, respectively.

$$\varepsilon = \frac{\beta\cos\theta}{4}. \quad (5)$$

Table 1. Structural parameters of vacuum deposited zinc telluride thin film.

Thickness of the film (t) in (nm)	Crystallite size (D) in (nm)	Number of crystallites (m^{-2})	Strain (ε) in lines-m^2	Dislocation density (ρ) lines/min^2	Lattice spacing (d) in Å	Lattice parameter (a) in Å
400	33.045	1.14×10^{16}	1.18×10^{-3}	9.16×10^{14}	2.82008	6.4689

$$\rho = \frac{1}{D^2}. \tag{6}$$

The crystallite size (D), strain (ε), dislocation density (ρ) and lattice spacing (d_{hkl}), lattice parameter (a) were estimated and are presented in table 1.

3.2 *Ordering parameter measurement*

In order to achieve better crystallinity and good environmental stability, high atomic order parameter is crucial for the investigation of thin films [27, 28]. The order parameter for a bulk material is calculated by measuring the X-ray integrated intensity ratio of a super lattice peak to a fundamental peak. Comparing this ratio to a theoretical value, order parameter can be calculated for a fully ordered sample, which can be expressed as

$$S = \left(\frac{I_s \times I_f^*}{I_f \times I_s^*}\right)^{\frac{1}{2}} \tag{7}$$

where S is the atomic order parameter whose value is between 0 (disorder) and 1 (fully ordered), the subscript s refers to the super lattice peak and the subscript f refers to the fundamental peak. I_f^* and I_s^* are the theoretically calculated peak intensities obtained for a fully ordered specimen, and I_f and I_s are the integrated peak intensities obtained from the experimental results for a sample whose order parameter is to be measured.

The theoretical relative integrated intensity from an XRD is usually expressed as

$$I = |F|^2 p\left(\frac{1+\cos^2 2\theta}{\sin^2\theta\cos\theta}\right) \tag{8}$$

where I is the relative integrated intensity (arbitrary units), F is the atomic structure factor, p is the multiplicity factor, and θ is the Bragg angle. The trigonometric terms in the parentheses are Lorentz polarisation factor. The intensity calculation is carried out in table 2, where f_{Te} and f_{Zn} are the atomic scattering factor [29] of tellurium and zinc, respectively. The order parameter can be obtained by measuring the X-ray integrated intensity ratio of the super lattice peak (1 1 1) and the fundamental peak (2 0 0). By comparing it to the theoretical value for a fully ordered sample, the order parameter of the ZnTe thin film has been obtained as 0.83.

3.3 *Surface morphology*

Atomic force microscope is used to check the surface morphology of the thin film. The surface roughness of the film can be measured by AFM, which is a measure of the texture of the film. Figure 3 shows the AFM images of ZnTe thin film annealed in vacuum at (a) 423 K, (b) 473 K, (c) 523 K and (d) 573 K, respectively, for 1 h. It is evident from figure 3 that the films are smooth and continuous. AFM images also revealed that the crystallinity of the film increases with increase in annealing temperature. These results are in good agreement with those resulting from XRD patterns (figure 2). The surface roughness estimated from the AFM images of the evaporated ZnTe films annealed at 423 K, 473 K, 523 K and 573 K was 1.11 nm, 2.27 nm, 2.81 nm and 3.08 nm respectively, indicating that roughness increases with increase in annealing temperature.

3.4 *Optoelectronic properties*

The optical properties of group II–VI semiconductor materials can be tuned by changing their structure or

Table 2. Intensity calculation of zinc telluride thin film.

Line	hkl	sin θ	θ	(sin θ /λ) (A^{-1})	f_{Te}	f_{Zn}	$\lvert F\rvert^2$	P	$\left(\frac{1+\cos^2 2\theta}{\sin^2\theta\cos\theta}\right)$	Relative integrated intensity: Theoretical value	Relative integrated intensity: Experimental value	Relative integrated intensity: Observation
1	111	0.206	11.93	0.134	45.78	25.48	43920	8	43.88475	15.419×10^6	15.13	Strong
2	200	0.220	12.73	0.143	45.14	25.04	6464	6	38.29313	1.4852×10^6	2.1	Strong
3	220	0.364	21.39	0.236	38.94	20.88	57254	12	12.41701	8.5312×10^6	2.7	Weak
4	311	0.395	23.31	0.256	37.76	20.12	29290	24	10.23446	7.1944×10^6	5.0	Strong

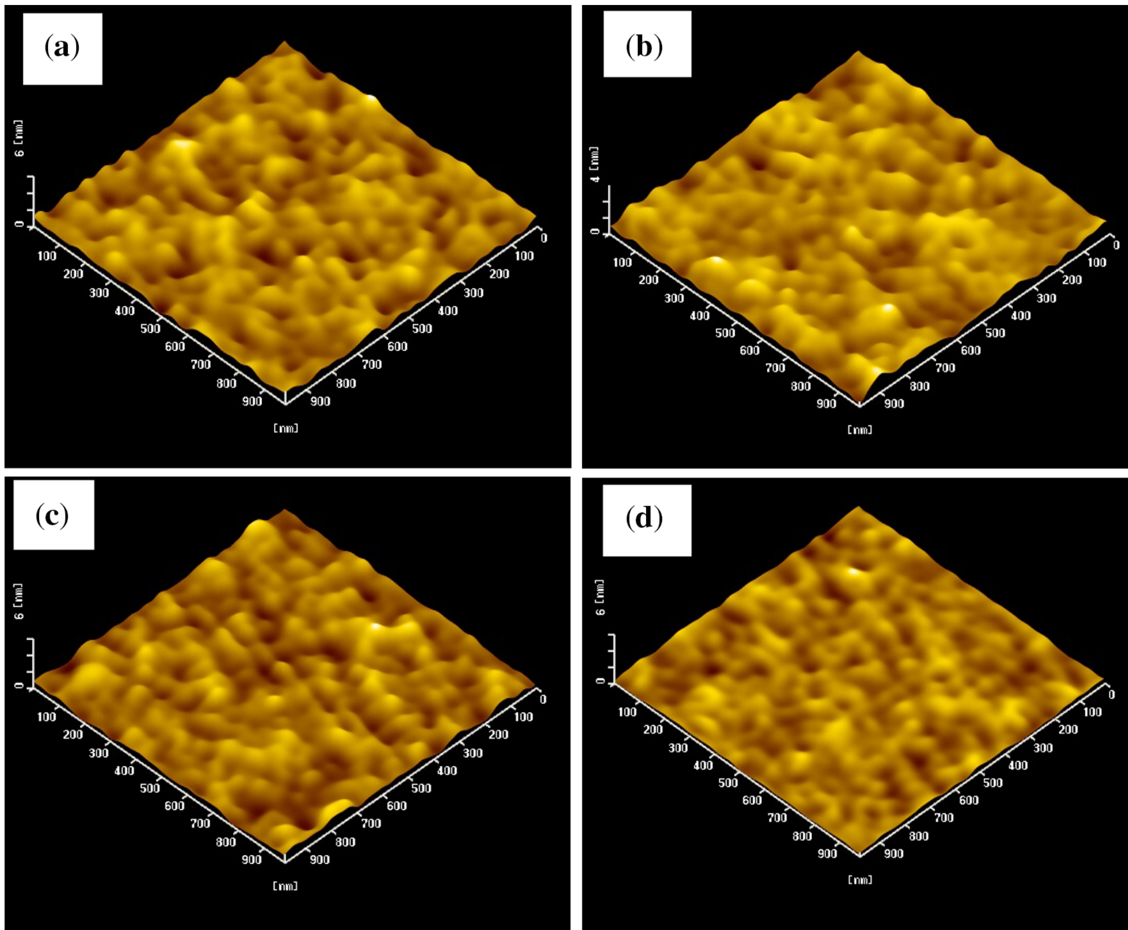

Figure 3. AFM images of vacuum evaporated ZnTe thin film annealed at (**a**) 423 K, (**b**) 473 K, (**c**) 523 K, and (**d**) 573 K respectively.

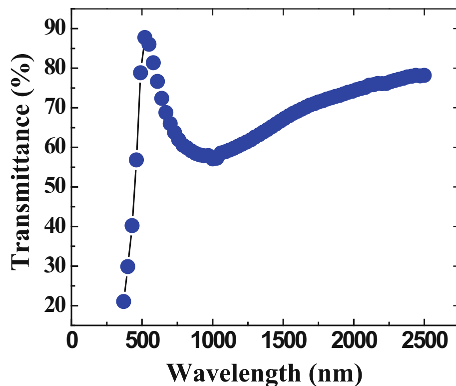

Figure 4. Optical transmission spectrum of ZnTe thin film annealed at 573 K.

composition. When two materials with different band structures meet, there will be an offset in the valence and conduction bands. This can significantly change the optical and electronic properties of the material, and allows further tailoring for the fabrication of devices. Figure 4 shows the optical transmittance spectrum of ZnTe thin film annealed at 573 K. The optical transmittance spectrum of this film was obtained from the UV-VIS-NIR spectrophotometer at room temperature in the wavelength range of 370–2500 nm. It is also found from figure 4 that the maximum transmittance of about 87.73% is obtained at a wavelength of 520 nm that can be attributed to the improvement in geometry and homogeneity of the film. The emergence of interference fringe in the transmission spectrum confirmed the excellent quality and homogeneity of ZnTe thin film. The transmittance of the film depends on the film thickness; the lower the thickness of the film, the higher the transmittance of the film and vice versa [30].

By applying the Swanepoel model [31], the optical parameters such as energy band gap and refractive index can be determined from the transmission spectrum. The optical thickness d was obtained from the following relation:

$$d = \frac{\lambda_{\max} \times \lambda_{\min}}{4n(\lambda_{\max} - \lambda_{\min})} \tag{9}$$

where n is the refractive index, $\lambda_{\max}$ is the maximum and $\lambda_{\min}$ is the minimum wavelength.

The refractive index n was obtained by using the relation

$$n = \frac{\left[N + (N^2 - 4s^2)^{\frac{1}{2}}\right]}{2} \tag{10}$$

where

$$N = 1 + s^2 + 4s\left(\frac{T_{max} - T_{min}}{T_{max} \times T_{min}}\right) \tag{11}$$

and s is the refractive index of glass, T_{max} is the maximum and T_{min} is the minimum transmittance. The refractive index of the film was calculated as 2.66 from the interference fringe of the transmittance spectrum. A porous film has a lower refractive index because air trapped in the pores of the film can effectively lower the refractive index. Post-deposition annealing eliminates the pores of the films, which considerably increases the refractive index, hence, enhances the crystallinity and density of the film.

The energy band gap for direct band-to-band transmission can be calculated by using Eq. (11) is given as follows:

$$\alpha h\upsilon = A(h\upsilon - E_g)^{\frac{1}{2}} \tag{12}$$

where A is a constant, $h\upsilon$ is the incident photon energy, and E_g is the energy band gap of the material. Therefore, a plot of $(\alpha h\upsilon)^2$ against $(h\upsilon)$ is expected to yield a straight line whose intercept with the energy axis measures the band gap energy as shown in figure 5. Using figure 5, an optical energy gap (E_g) of 2.67 eV was obtained from the vacuum-evaporated ZnTe thin film. This value is in good agreement with the value reported in literature (2.62–3.24 eV) for vacuum-evaporated films [15]. The absorption coefficient (α) was estimated using the following relation [30]:

$$\alpha = \frac{4\pi k_\lambda}{\lambda} \tag{13}$$

where k_λ is the extinction coefficient, which is calculated from the following relation:

$$k_\lambda = \frac{\ln(1/T)\lambda}{4\pi d} \tag{14}$$

where T is the transmittance, d is the film thickness and λ is the incident photon wavelength. The absorption coefficient and the extinction coefficient are plotted against the wavelength (λ) and the photon energy ($h\upsilon$). The absorption coefficient (α) and extinction coefficient (k) are depicted in figures 6 and 7, respectively. It has been observed from figure 6 that at the photon energy of 2.5 eV there is a sharp increase in absorption coefficient near the band-gap region. Compounds with higher absorption coefficients absorb photons more readily, which enhanced the excitation of electrons into the conduction band. The absorption coefficients of materials help the engineers in determining which material is suitable for their solar cell designs. From figure 7, it is evident that the extinction coefficient of ZnTe thin film sharply increased from visible to near-infrared region, which justifies the possibility of using this film as window layers in heterojunction thin-film-based solar cells.

Figure 8 shows the room temperature optical absorption spectrum of ZnTe thin film in the wavelength range of 400–600 nm. Figure 8 shows that a strong absorption peak

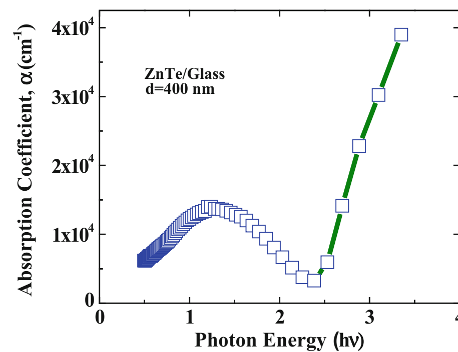

Figure 6. Photon energy dependence absorption coefficient (α) of ZnTe thin film annealed at 573 K.

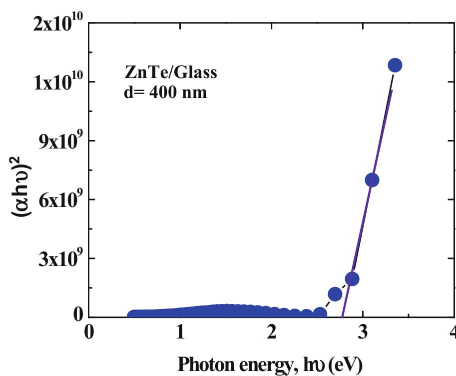

Figure 5. Determination of band gap energy from $(\alpha h\upsilon)^2$ versus $(h\upsilon)$ plot for ZnTe thin film annealed at 573 K.

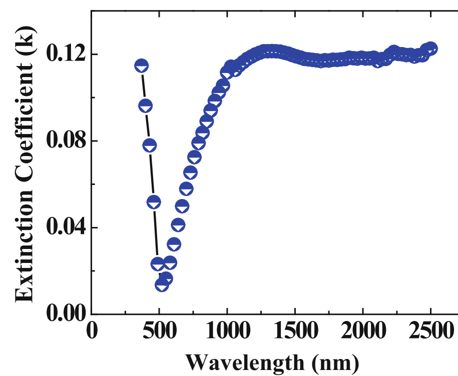

Figure 7. Wavelength dependence extinction coefficient (k) of ZnTe film annealed at 573 K.

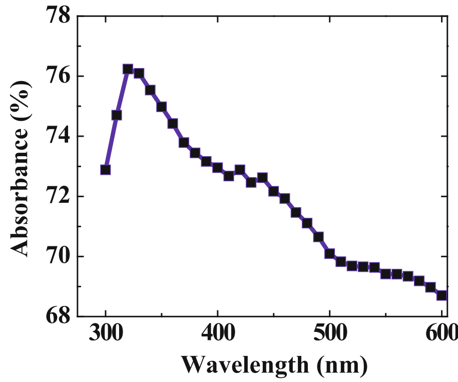

Figure 8. Absorbance spectrum of ZnTe thin film annealed at 573 K.

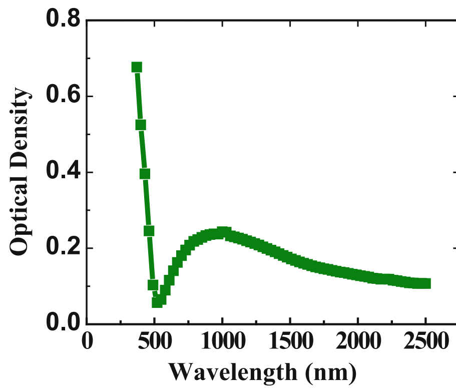

Figure 9. Optical density of ZnTe thin film annealed at 573 K.

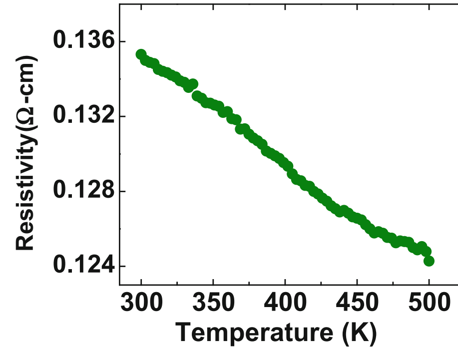

Figure 10. Temperature dependence electrical resistivity of ZnTe thin film annealed at 573 K.

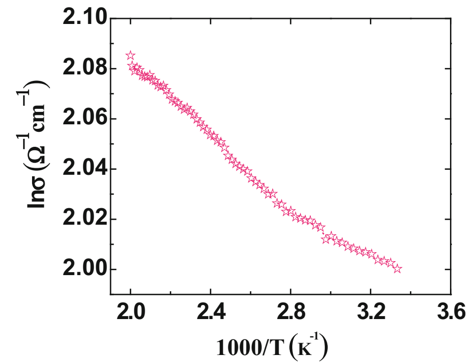

Figure 11. Electrical conductivity of ZnTe thin film annealed at 573 K.

appears in the UV region at a wavelength of 320 nm. The absorption of photons creates both majority and minority carriers. The basis of the photovoltaic fabricated energy is the generation of charge carriers by photons. The higher the peak, the more ZnTe there is per unit sample of the film.

The optical density, which is a measure of the transmittance of an optical medium for a given wavelength, was calculated from transmittance data using the following relation [32]:

$$OD = \log_{10}\frac{1}{T}. \quad (15)$$

Note that when the optical density of a medium is high, then the transmittance of that medium is low, and vice versa. Optical density is related to the refractive index (n) of a material; a higher value of refractive index means higher optical density. Figure 9 shows the optical density of ZnTe thin film with respect to the wavelength. It is apparent from this figure that the optical density is higher at a lower wavelength and it rapidly decreased with increase in wavelength.

3.5 *Electrical properties*

In order to understand the electrical properties of the vacuum-evaporated ZnTe thin film, it is essential to know the resistivity and conductivity of the prepared film. Figure 10 shows the temperature-dependence of electrical resistivity of the ZnTe thin film. It is well known that low resistivity is favorable for ohmic contact. It is evident from figure 10 that the resistivity is decreasing with increase in temperature, which is the characteristic property of semiconductors (the increase in the number of free electron is associated with the electrical conductivity in semiconductor materials). Hence, at a low temperature range (300–500 K), the temperature dependence of mobility would generally be small in comparison with that of the hole density. Therefore, temperature dependence of conductivity can be approximated by that of the hole density, p; i.e., $p \propto \exp(\Delta E/kT)$. The result obtained in this way is in good agreement with the previously reported literature value [33]. Since mobility and conductivity are directly related and conductivity and resistivity are inversely related, hence, with the increase in carrier mobility, resistivity decreases or conductivity increases [34]. The plot of the lnσ versus 1000/T for ZnTe thin film is shown in figure 11. It is

observed from this figure that the conductivity changes rapidly with temperature. This result indicates that the conduction mechanism observed here is due to thermally assisted tunneling of charge carriers in the localised states in band tails. The result obtained for ZnTe thin film is in good agreement with the previously reported literature value [24].

Finally, we have compared the properties of our vacuum-evaporated ZnTe thin film with previously reported results. Pattar *et al* [35] studied the structural, optical and electrical properties of vacuum-evaporated indium-doped ZnTe thin films. They observed that doped films were found to exhibit two diffraction peaks associated with (1 1 1) and (2 2 0), of which the intensity of (1 1 1) orientation is predominant. They revealed that there is a slight decrease in absorbance for the doped films due to the incorporation of indium atoms into the film. However, the optical band gap of doped films decreased with the increase in doping concentrations, which is the main purpose of doping. As compared with this result, we have obtained four diffraction peaks with improved intensity for undoped ZnTe thin film with crystallite size of 33.045 nm, micro strain (ε) of 1.18×10^{-3} ($\mathrm{lin}^{-2}\ \mathrm{m}^{-4}$) and dislocation density (ρ) of 9.16×1014 ($\mathrm{lin/min}^2$) with optimum band gap. Jeetendra [36] and co-workers have studied the concentration-dependent optical and structural properties of molybdenum (Mo)-doped ZnTe thin films prepared by e-beam evaporation method. They showed that the crystallite size decreased up to 14.579 nm with increase in doping concentration, and the strain and dislocation density increased continuously up to 2.482 ($\mathrm{lin}^{-2}\ \mathrm{m}^{-4}$) and 4.704×10^{15} ($\mathrm{lin/m}^2$), respectively, for 25 wt% of ZnTe:Mo, with decrease in optical energy band gap. They also found that the optical transmittance was decreased with a range of 14–8% in the wavelength range of 700 nm to 900 nm, with increase in doping concentration from 5 wt% to 25 wt%. In the present study, we have obtained the maximum transmittance of about 87.73% at the wavelength of 520 nm and comparatively better result achieved in the wavelength range of 1000 nm to 2500 nm for undoped ZnTe thin film. John *et al* [37] also studied copper-doped ZnTe thin films and showed that the XRD studies have not revealed any change in the film structure of the as-deposited and copper (Cu)-doped samples. They have noticed that the transmission is reduced due to doping of Cu in ZnTe films. But, in our present study, a maximum optical transmittance of about 87.73%, a refractive index of 2.66 and the crystallite size of 32.045 nm were obtained for undoped ZnTe thin film.

4. Conclusions

ZnTe thin film was deposited on glass substrate by thermal vacuum evaporation (TVE) technique. XRD studies revealed that the sample is polycrystalline with cubic structure. Order parameter, crystallite size, microstrain, dislocation density, lattice parameter and lattice spacing were calculated from the XRD data. Morphological investigation of the film was carried out using AFM, which gives the surface roughness of the film. The XRD results also support the AFM investigation. The optical study indicated a band-to-band transition with a band gap of 2.63 eV. Transmittance, optical thickness, refractive index, extinction coefficient and absorption coefficient have also been investigated here. The electrical properties have been studied in the temperature range of 300–500 K, where conduction is due to thermally assisted tunneling of the charge carriers and confirmed the semiconducting nature of the film. Different characteristics studies of ZnTe performed in this paper revealed the motivation for further studies in the field of solar energy-to-electricity conversion.

Acknowledgements

Part of this work was carried out in the Materials Science Division, Atomic Energy Center, Dhaka, Bangladesh. The authors are grateful to the concerned authority and laboratory staff of Bangladesh Council of Scientific and Industrial Research (BCSIR) and Bangladesh University of Engineering and Technology (BUET) for their support, cooperation and technical assistance in experimental measurements.

References

[1] Swank R K 1967 *Phys. Rev.* 153: 844
[2] Bhargava R 1995 *Properties of wide band gap II–VI semiconductors* (Institution of Engineering & Technology)
[3] Rohatgi A, Ringel S A, Sudharsanan R, Meyers P V, Liu C H and Ramanathan V 1989 *Solar Cells* 27: 219
[4] Tanaka T *et al* 2010 *J. Appl. Phys.* 108: 502
[5] Feng X, Singh K, Bhavanam S, Palekis V, Morel D L and Ferekides C S 2012 *38th IEEE Photovoltaic Specialists Conference (PVSC)*
[6] Gessert T A *et al* 2013 *Thin Solid Films* 535:237
[7] Guo Q *et al* 2007 *Solid State Commun.* 141: 188
[8] Padiyan D P, Marikani A and Murali K R 2003 *Mater. Chem. Phys.* 78: 51
[9] Glew R W 1977 *Thin Solid Films* 46: 59
[10] Kissinger N J S, Jayachandran M, Perumal K and Raja C S 2007 *Bull. Mater. Sci.* 305: 47
[11] Gopakumar N, Anjana P S and Vidyadharan Pillai P K 2010 *J. Mater. Sci.* 45: 6653
[12] Baron T, Saminadayar K and Magnea N 1998 *J. Appl. Phys.* 83: 1354
[13] Melo O D, Larramendi E M, Duart J M M, Velez M H, Stangl J and Sitter H 2007 *J. Cryst. Growth* 307: 253
[14] Erlacher A *et al* 2005 *Appl. Surf. Sci.* 248: 402
[15] Seyam M A M 2012 *J. Alloys Compounds* 541: 448
[16] Christen H M and Eres G 2008 *J. Phys.: Condens. Matter* 20: 264005
[17] Bellakhder H, Outzourhit A and Ameziane E L 2001 *Thin Solid Films* 382: 30

[18] Ibrahim A A, El-Sayed N Z, Kaid M A and Ashour A 2004 *Vacuum* 75: 189
[19] Kazmerski L L, Ayyagani M S, White F F and Sanborn G A 1976 *J. Vacc. Sci. Technol.* 13: 139
[20] Ahamed J U, Sanbongi T, Katano S and Uehara Y 2010 *Jpn J. Appl. Phys.* 49: 08LB09
[21] Yang T R and Lu C C 2000 *Physics B* 284: 1187
[22] Ahamed J U, Katano S and Uehara Y 2016 *Trans. Ind. Inst. Met.* 69: 1579
[23] Alam A J and Cameron D C 2000 *Thin Solid Films* 377–378: 455
[24] Kumar B R, Hymavathi B and Rao T S 2014 *Chalcogenide Lett.* 11: 509
[25] El-Kadry N, Ashour A and Mahmoud S A 1995 *Thin Solid Films* 269: 112
[26] Mahalingam T, John V S, Ravi G and Sebastian P J 2002 *Cryst. Res. Technol.* 373: 29
[27] Farrow R F C, Weller D, Marks R F, Toney M F, Cebollada A and Harp G R 1996 *J. Appl. Phys.* 79: 5967
[28] Yang B, Asta M, Mryasov O N, Klemmer T J and Chantrell R W 2006 *Acta Mater.* 54: 4201
[29] Culity B D 1956 *Elements of X-ray diffraction*, second edition, pp. 126–143
[30] Potlog T, Maticiuc N, Mirzac A, Dumitriu P and Scortescu D 2012 *IEEE Trans. Semicon.* 2: 321
[31] Swanepoel R 1983 *J. Phys. E: Sci. Instrum.* 16: 12
[32] Mahmood W, Shah N A, Akram S, Mehboob U, Malik U S and Sharaf M U 2013 *Chalcogenide Lett.* 10: 273
[33] Ishizaki T, Ohtomo T and Fuwa A 2004 *J. Phys. D: Appl. Phys.* 37: 255
[34] Farooq M U, Khan M, Faraz A, Maqsood A, Ahmad W and Li L 2014 *Maters. Tech.: Adv. Perform. Maters.* 29: 29
[35] Pattar J, Sawant S N, Nagaraja M, Shashank N, Balakrishna K M, Sanjeev G and Mahesh H M 2009 *Int. J. Electrochem. Sci.* 4: 369
[36] Jeetendra S, Nagabhushana H, Mrudula K, Naveen C S, Raghu P and Mahesh H M 2014 *Int. J. Electrochem. Sci*. 9: 2944
[37] John V S, Mahalingam T and Chu J P 2005 *Solid-State Electron.* 49: 3